ISTITUTO NAZIONALE DI FISICA NUCLEARE

Sezione di Milano

INFN/BE-89/7
22 Dicembre 1989

E. Gadioli , E. Gadioli Erba:

NUCLEON-NUCLEON INTERACTIONS IN HEAVY ION REACTIONS

Invited talk delivered at the
"LXXV National Congress of Italian Physical Society"
Cagliari (1989)

Servizio Documentazione
dei Laboratori Nazionali di Frascati

INFN - Istituto Nazionale di Fisica Nucleare
Sezione di Milano

INFN/BE-89/7
22 Dicembre 1989

NUCLEON-NUCLEON INTERACTIONS IN HEAVY ION REACTIONS

ETTORE GADIOLI and ENRICA GADIOLI ERBA
Dipartimento di Fisica, Universitá di Milano
Istituto Nazionale di Fisica Nucleare, Sezione di Milano
via Celoria 16, 20133 Milano, Italia

The phenomenology concerning the emission of fast nucleons in fusion and quasi-fusion reactions of two heavy ions is reviewed together with some of the theories developed to account for these processes. It is shown that, at energies exceeding ≈20 MeV/nucleon, nucleon-nucleon collisions play a major role in the equilibration process of the excited intermediate created in the interaction of the two ions. Some theoretical results predict a considerable hardening of the primary nucleon spectrum when the asymmetry parameter $y = A_p/A_T$ is sufficiently high.

In this paper we will limit ourselves to discussing the phenomenology concerning fusion and quasi-fusion reactions and, in particular, that referring to fast nucleon emission, to which interactions between projectile and target nucleons, when they come in strict contact, contribute in a significant way.

Many experiments focusing on these processes have been made at rather low incident particle energy ($\leq$ 10 MeV/nucleon) and have been interpreted assuming that the excited nucleus, after fusion with all or part of the projectile, mainly de-excites by nucleon evaporation.

At higher incident energies ($\geq$ 20 MeV/nucleon) information on pre-equilibrium emission mainly comes from the study of the spectra of light ejectiles.

Fig. 1 shows the experimental differential multiplicities of neutrons from the interaction of 300 MeV ^{12}C ions with ^{165}Ho, measured in coincidence with an evaporation residue emitted at a forward angle (Holub *et al* 1986). The results of such experiments look rather similar to the pre-equilibrium + equilibrium spectra measured in the case of nucleon induced reactions. In spite of this, these spectra are often parametrised in terms of isotropic statistical emissions from two (or more) moving sources. One of these fits is shown in the figure by the continuous lines that are given by the incoherent addition of two contributions: the first, referring to evaporated neutrons, corresponds to emissions from a source moving in the beam direction with a velocity equal to that of the two ion center of mass, the second, corresponding to the fast component of the spectrum, from a source moving in the beam direction with a velocity about one half of the beam velocity, which corresponds to the mean velocity of the nucleon-nucleon center of mass.

This parametrisation has been used to fit most of the inclusive and exclusive data reported in the literature (see for instance, Awes *et al* (1981, 1982), Glasow *et al* (1983), Holub *et al* (1983a,1986), Hilscher *et al* (1987)) and might provide evidence in favor of theoretical models that interpret the light particle spectra as originating from isotropic emissions from high temperature hot-spots corresponding to the zone of the di-nuclear system where the projectile and the target density distributions come

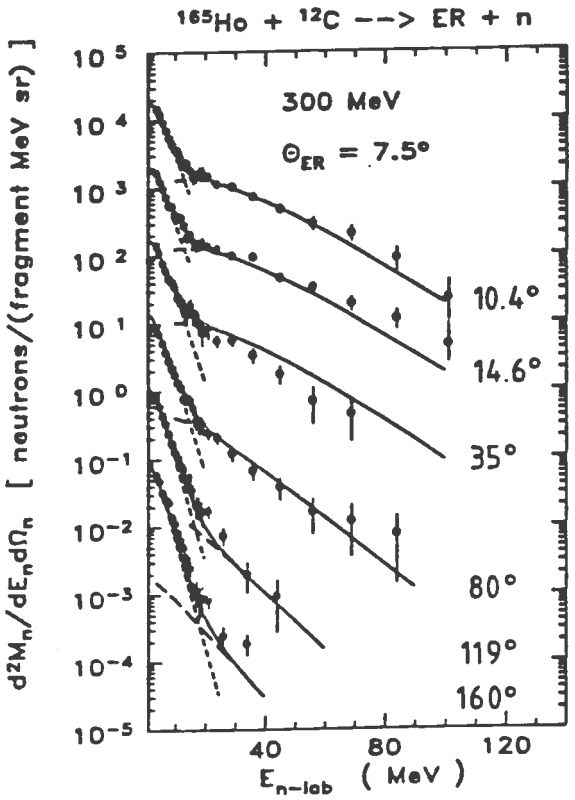

Fig. 1

Measured double differential cross-sections of neutrons from the reaction ^{12}C(^{165}Ho, nX) at 300 MeV (black points) measured in coincidence with evaporation residues having velocity larger than 0.23 cm/ns, detected at 7.5°. The full line are the result of the moving source parametrisation described in the text (Holub *et al* (1986).

in contact. Nucleons with the energy distribution expected for an high temperature Fermi gas might cross the boundaries of the hot spot leaving the di-nuclear system either immediately or after a propagation in the cold surrounding regions. The existence of the hot spot requires that in its interior the nucleon mean free path be very short so that nucleon-nucleon collisions lead very rapidly to a thermalisation. On the other hand, in the cold surrounding regions the nucleon mean free path is assumed to be very long allowing the propagation of the fast nucleons coming from the hot spot without any interaction that could reduce their energy (Morison *et al* 1980). Though these requirements might, at least qualitatively, be justified by theoretical predictions of the dependence of the mean free path of a nucleon on the temperature of the nuclear matter through which it propagates (Collins and Griffin 1980), it is doubtful if they can be really satisfied in practice.

At energies of some ten MeV/nucleon, the parametrisation of light particle spectra in terms of isotropic emissions from moving sources is by no means the only way to reproduce the data. Korolija *et al* (1988a,b) first remarked that a very accurate reproduction of the measured proton differential cross-sections, in heavy ion reactions at $\approx$20 MeV/nucleon, may be obtained by a multi-source fit including a non-isotropic emission from a source moving with the two ion center of mass velocity. Fig. 2 shows the fit to inclusive proton differential spectra (in reactions induced by S ions on ^{124}Sn and Au) obtained by considering contributions from four sources, three of which represent isotropic emissions from, respectively, the composite nucleus (evaporations at the end of a pre-equilibrium cascade), a source simulating a fast projectile-like fragment and a source simulating a slow target-like fragment (the velocities of these last two sources are free parameters whose value is obtained by a best fit procedure). The fourth contribution represents forward emissions from a non-equilibrated source moving with the composite nucleus velocity. The degree of anisotropy in this source system is characterised by $\Delta\theta$ that, as shown by Mantzouranis *et al* (1976), represents the intrinsic uncertainty in the direction of a nucleon due to the finite size of the

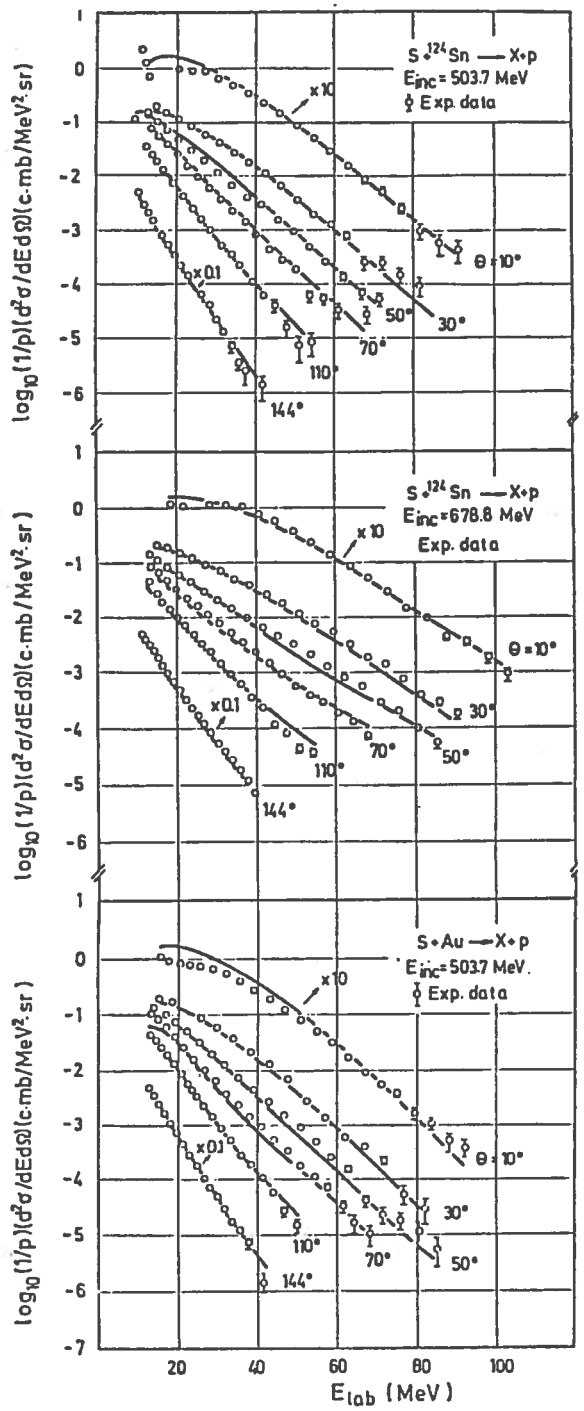

Fig. 2

Moving source parametrisation of experimental proton differential cross-sections using four moving sources, one accounting for pre-equilibrium emissions from the composite system (Korolija *et al* 1988b)

emitting source and is given by

$$\Delta\theta \approx \frac{2\pi}{kR_{CN}}, \tag{1}$$

k being the nucleon wave number and R_{CN} the source radius (in this case the composite nucleus radius). The forward peaked angular distribution is suggested to be given by

$$\sigma(\theta, E) \propto \exp(-\theta/\Delta\theta(E)) \tag{2}$$

which, in fact, as shown in Fig. 3, reproduces rather satisfactorily the average θ dependence of the estimated pre-equilibrium contribution to the CM double differential spectra of nucleons emitted in fusion processes (Fabrici *et al* 1989a).

Fig. 4 shows the various contributions to the angle-integrated cross-section in the case of the reaction ^{124}Sn(S,pX) at 678.8 MeV.

When one studies theoretically the interaction between two heavy ions to reproduce single-particle observables, one must consider either the action of the mean-field (that acts on the nucleons and changes as the two ions move one against the other, stick together and eventually fuse or separate again) and the effects of nucleon-nucleon collisions due to the residual interaction that are most effective in producing a sharing of the nucleon energies and momenta. At low incident energies, it is expected that residual interactions are of little importance due to the Pauli blocking. At the increase of the relative energy of the two ions, the restrictions due to the Pauli principle become less effective and the importance of the nucleon-nucleon interactions grows. Finally at high relative energies the interaction between the two heavy ions should be essentially describable in terms of nucleon-nucleon collisions.

The most sophisticated way to treat mean-field effects is by using the time-dependent Hartree-Fock (TDHF) theory (Negele 1982 and Davies *et al* 1984). However in most of these calculations, due to the great mathematical and computational complexity, the residual interactions are neglected compared with the mean-field. When the residual interactions are important one can use approximations, some of which are described in the following.

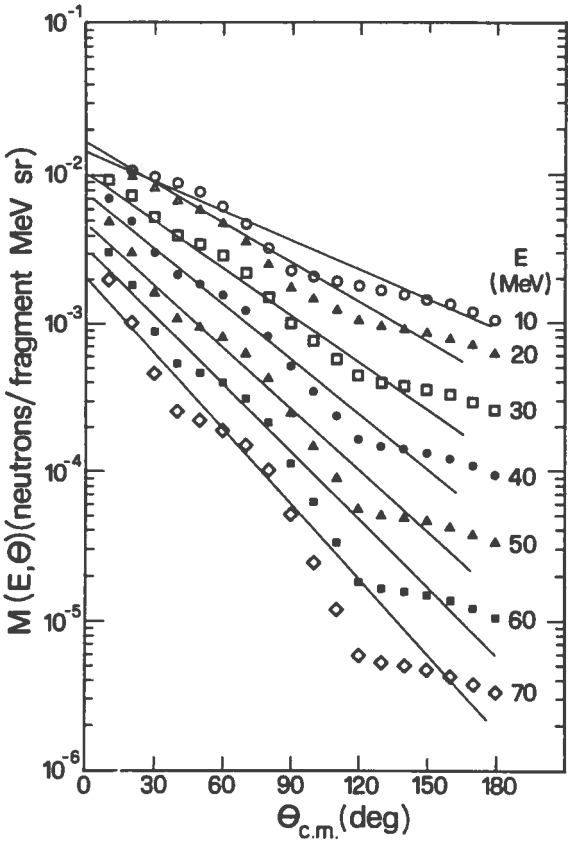

Fig. 3

Double differential centre of mass multiplicity distributions of neutrons from 300 MeV ^{12}C bombardment of ^{165}Ho. The experimental multiplicities are given by open and full dots, triangles, squares and diamonds. The full lines show the expression $M(\theta, E) \propto \exp(-\theta/\Delta\theta(E))$ with $\Delta\theta = 2\pi/kR$, where k is the neutron wave number and R the radius of the composite nucleus (Fabrici *et al* 1989a).

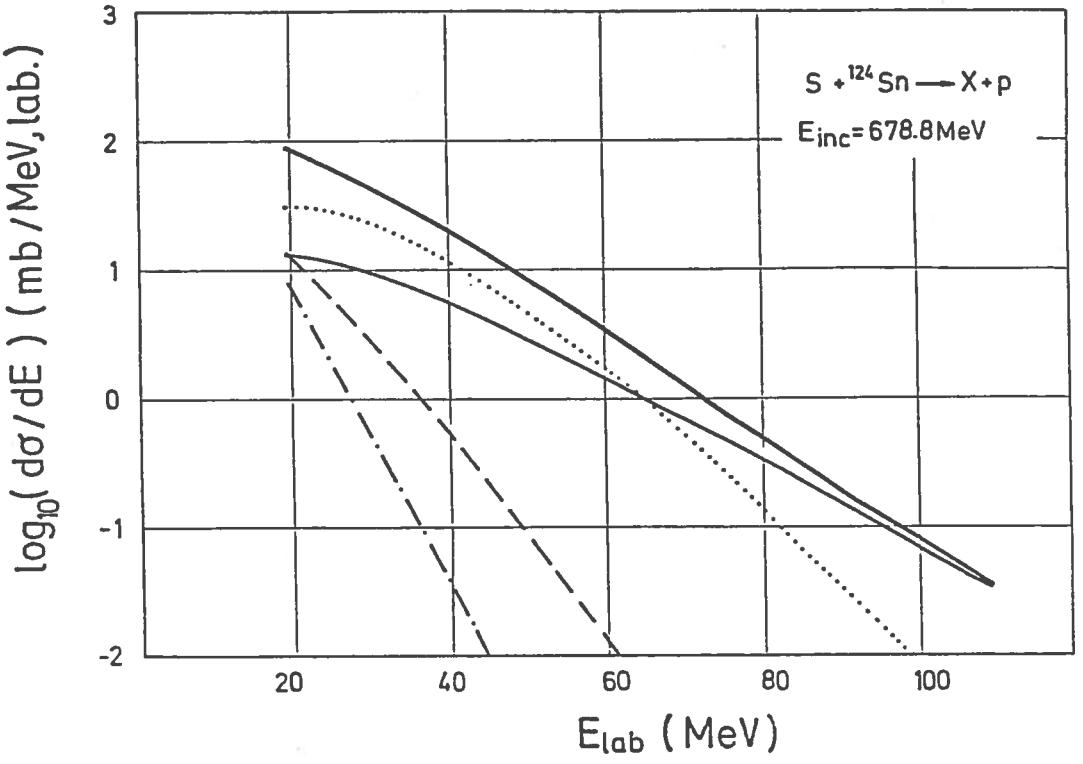

Fig. 4

Contributions to the total angle-integrated cross-section for proton production in the reaction ^{124}Sn(S,pX) at 678.8 MeV (thick solid line): dashed line, compound nucleus evaporations; dotted and dash-dotted lines, projectile-like and target-like emissions; thin solid line, pre-equilibrium emissions from the composite nucleus (Korolija *et al* 1988b)

The first consists in evaluating the single particle phase space distribution f(r,p,t) by means of the Vlasov-Uehling-Uhlenbeck (VUU) equation

$$\frac{\partial f_1}{\partial t} + \mathbf{v} \cdot \frac{\partial f_1}{\partial \mathbf{r}} - \Delta U \cdot \frac{\partial f_1}{\partial \mathbf{p}} = - \int \frac{d^3\mathbf{p}_2 d^3\mathbf{p}_{1'} d^3\mathbf{p}_{2'}}{(2\pi)^6} \sigma v_{12} [f_1 f_2 (1 - f_{1'})(1 - f_{2'}) +$$

$$- f_{1'} f_{2'} (1 - f_1)(1 - f_2)] \delta^3(p_1 + p_2 - p_{1'} - p_{2'}), \qquad (3)$$

where U is the mean-field potential which is assumed to be a specified function of the local density (Aichelin and Bertsch 1985).

With the right-hand side set to zero this equation reduces to the Vlasov equation which is the classical analogue of the TDHF equations. It has been shown that, at incident energies greater than $\approx$ 25 MeV/nucleon the Vlasov equation is a good approximation to the quantum mechanical TDHF theory (Aichelin and Bertsch 1985, Kruse *et al* 1985, Aichelin 1986).

The right-hand side term of (3) accounts for the two-body collisions and has a structure similar to that of the Boltzmann master equations proposed by Harp, Miller and Berne (1968) to describe the nuclear relaxation in the course of a cascade of nucleon-nucleon interactions. It is a sum of a feeding and a depletion contribution and the effect of Pauli blocking is simulated by the $(1 - f)$ factors appearing within the square brackets. Indices 1,2,1′,2′ refer to the collision partners before and after the interaction.

To solve the VUU equation, one uses a numerical method from hydrodynamics (Aichelin and Bertsch 1985). The phase space is divided into cells and the phase space distribution function is represented by a collection of test particles whose coordinates evolve individually. For evaluating quantities depending on the phase space density, such as the potential field or the Pauli operators $(1 - f)$, the number of test particles within each cell is counted.

The solution of the Vlasov equation is obtained by computing the dynamical evolution of the test particles by Newtonian mechanics. The initial phase space distributions are those corresponding to particles distributed uniformly in spheres with radius $r_o A^{1/3}$ with momenta given by a local Fermi gas approximation, assuming

that the spheres representing the nuclei in momentum space are displaced from each other by their relative momenta.

The collision integral is evaluated in a stochastic way assuming that two particles may interact if they approach each other to a distance smaller than $\sqrt{\sigma/\pi}$ and if the scattering is not Pauli blocked.

Without entering further in computational details we may discuss only a few results.

In Fig. 5 are compared the coordinate-space time evolutions predicted for the single particle distribution functions, in the case of the interaction of C ions at an energy of 84 MeV/nucleon and a small impact parameter (b=1 fm), as predicted by TDHF (without nucleon-nucleon collision terms), left, by the Vlasov equation, middle, and the VUU equation, right (Aichelin 1986). Both mean-field calculations display a remarkable transparency, while this is greatly reduced by considering nucleon-nucleon collisions that also greatly increase the probability of nucleon emissions.

Fig. 6 shows the momentum space time evolution of the single particle distribution functions in the case of a central collision (b=0 fm) for another symmetric system: Ar + Ca at 137 MeV/nucleon (Kruse *et al* 1985). One finds that the momentum space distribution is practically unchanged in the mean field calculation, while the inclusion of the collision term results in a strong thermalisation of the composite system.

According to these calculations in a typical heavy ion interaction, at an incident ion energy of some tens MeV, fast particle emission occurs at an early stage of the process (within about 10^{-22} sec$\approx$ 30 fm/c) with maxima in forward and backward direction in the case of symmetric heavy ion collisions and mainly in the forward direction in the case of asymmetric interactions. These particles mainly come from the overlap region where collisions occur between projectile and target nucleons. This is qualitatively what is expected on the basis of the PEP and Fermi jet theories (Bondorf *et al* 1980 and Robel 1979) where one predicts that nucleon emission in the forward (backward) direction is essentially due to projectile (target) nucleons, from the overlap region, having momenta equal to the sum of a forward (backward)

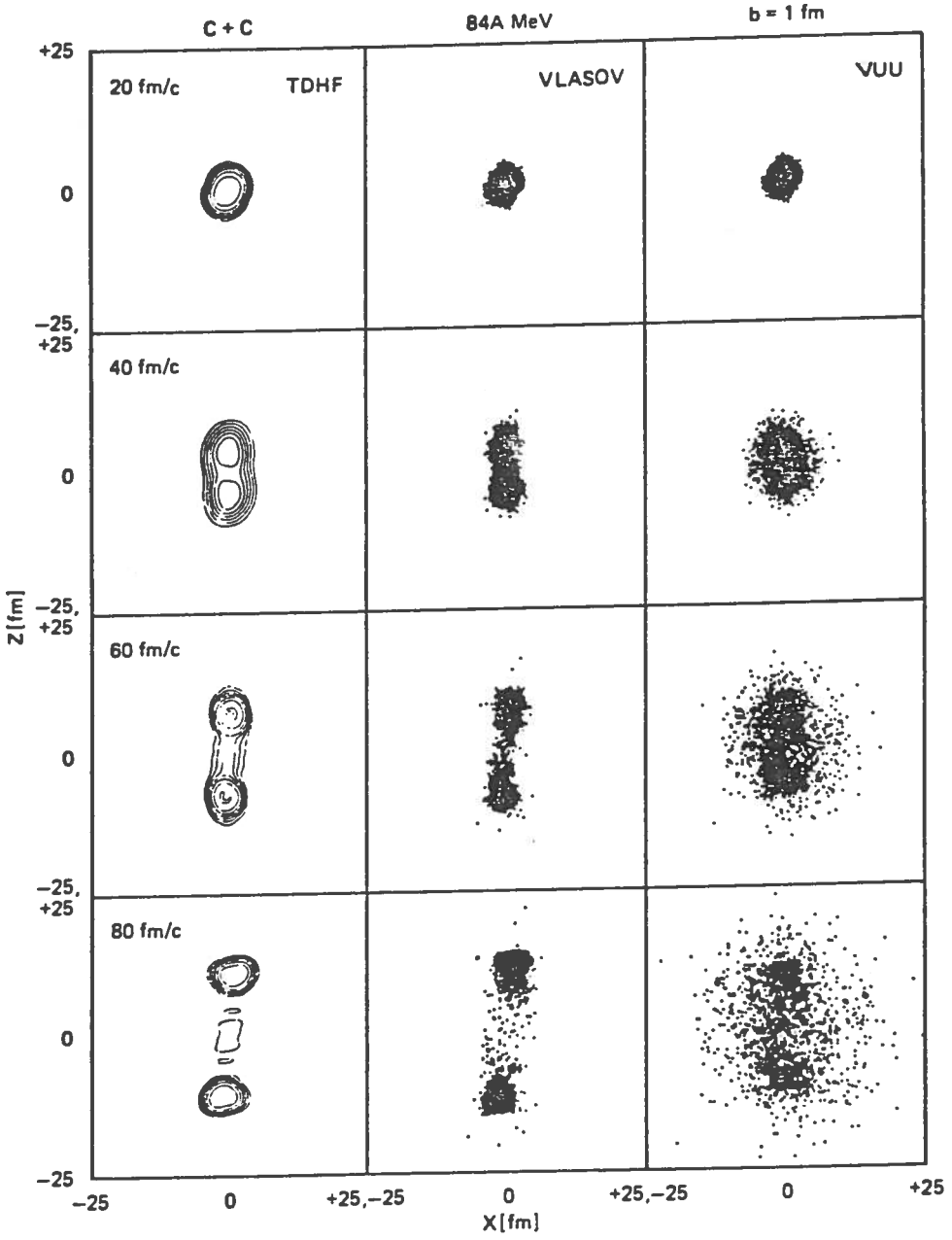

Fig. 5

Time evolution of the coordinate space single particle distribution functions for the symmetric system C+C at 85 MeV/nucleon and an impact parameter of 1fm (Aichelin 1986).

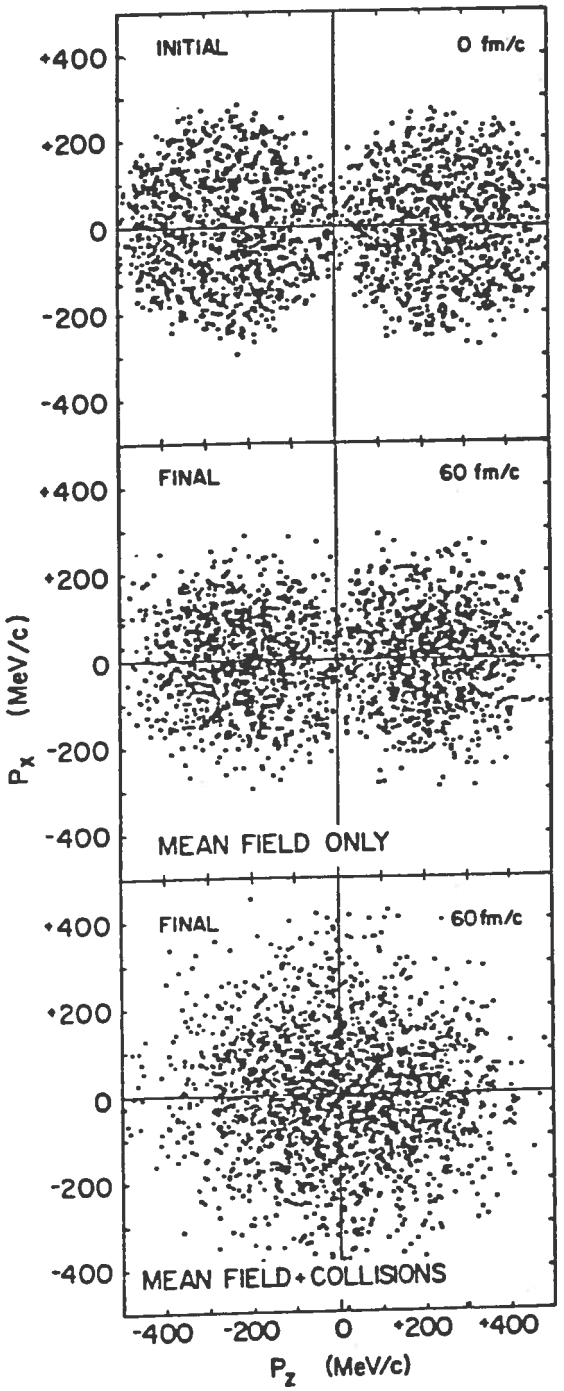

Fig. 6

Time evolution of momentum space single particle distribution functions for the near symmetric system Ar+Ca at 137 MeV/c. The case considered is that of a central collision (b=0 fm) (Kruse *et al* 1985).

directed translational momentum and a randomly directed Fermi-gas momentum that propagate through the nuclear matter, sometimes without interactions, sometimes suffering interactions with target nucleons. However, Aichelin (1986) found that the mean field interaction, in VUU theory, provides them with an extra push that increases their energy. This because the absorption of the projectile generates a region of density higher than normal and the mean field tends to lower the density in this region by accelerating particles towards lower density regions.

VUU theory, however, is semiclassical in nature, and violates the uncertainty principle. A way to improve this kind of calculation while retaining its physical assumptions has been indicated by Cassing (1987a, b, 1988). Cassing separates in time the action of the mean field and of the nucleon-nucleon interactions. The mean field interaction is dominant for $t \leq t_o$ and thereafter the time evolution is ruled by nucleon-nucleon interactions. The time

$$t_o = t_c + \tau/2, \tag{4}$$

where t_c is the time spent by the two nuclei to come in contact, and τ is the average primary nucleon-nucleon collision time which is estimated to be of the order of 10 fm/c at incident energies between 20 and 100 MeV/nucleon. The mean field interaction is evaluated by the TDHF theory and provides an average momentum-space distribution $f_{av}(\mathbf{k}, t=0)$ for nucleons in the overlap interaction region, whose subsequent time evolution depends on nucleon-nucleon interactions and emissions to the continuum.

The equilibration through two-body collisions and the emissions to the continuum are described by a system of master equations that, to avoid violation of uncertainty principle, evaluate the time evolution of the single nucleon momentum space distribution without considering explicitly the spatial coordinates:

$$\frac{\partial}{\partial t} f_{av}(\mathbf{k},t) = \frac{2\hbar^3}{M^2\pi^3} \int\int\int d^3q_2 d^3q_1' d^3q_2' \times$$

$$\frac{d\sigma(\mathbf{k}-\mathbf{q}_2, \mathbf{q}_1'-\mathbf{q}_2')}{d\Omega} \delta_3(\mathbf{k}+\mathbf{q}_2-\mathbf{q}_1'-\mathbf{q}_2') \delta\left(\frac{\hbar^2}{2M}(k^2+q_2^2-q'^2_1-q'^2_2)\right)[f_{av}(\mathbf{q}_1',t) f_{av}(\mathbf{q}_2',t) \times$$

$$(1 - f_{av}(\mathbf{k},t))(1 - f_{av}(\mathbf{q}_2,t)) - f_{av}(\mathbf{k},t)f_{av}(\mathbf{q}_2,t)(1 - f_{av}(\mathbf{q}'_1,t))(1 - f_{av}(\mathbf{q}'_2,t))]+$$

$$-\tau_f(\mathbf{k},t)^{-1} f_{av}(\mathbf{k},t) H[t - \tau_f(\mathbf{k},0)] H[\frac{\hbar^2 k^2}{2M} - U_o]. \qquad (5)$$

the quantities $\mathbf{k}$, $\mathbf{q}_2$,$\mathbf{q}'_1$,$\mathbf{q}'_2$ are the momenta of the interacting nucleons before and after scattering, U_o is the depth of the mean field and the H's are the Heaviside functions equal to unity for positive argument and zero otherwise.

The initial momentum space distribution $f_{av}(\mathbf{k}, t = 0)$ (as well as the time evolving one) contains high momentum components, essentially due to finite size effects, that are not possessed by distributions evaluated with use of Fermi gas model. Cassing (1988) claims that this quantum mechanical effect is of the greatest importance to reproduce the hardest part of emitted nucleon spectra.

The average time $\tau_f(\mathbf{k},t)$ during which a nucleon of momentum $\mathbf{k}$, in the rest frame of the moving mean field, experiences two-body collisions before reaching the di-nuclear surface with a chance to be emitted is given by the average distance of the nucleon from the surface divided by the nucleon velocity. Its reciprocal $\tau_f(\mathbf{k},t)^{-1}$ is tentatively taken to be the decay rate for emission to the continuum. The momentum distribution of particles in the continuum at time t is then

$$f_c(\mathbf{k},t) = \int_0^t \tau_f(\mathbf{k},t')^{-1} f_{av}(\mathbf{k},t') H[t' - \tau_f(\mathbf{k},0)] H[\frac{\hbar^2 k^2}{2M} - U_o] dt'. \qquad (6)$$

After the transformation to the energy and angles in the lab. system (E and Ω), one gets the spectrum of particles emitted with a given energy and direction up to time t in the lab system, $f_{lab}(E,\Omega,t)$. To obtain absolute cross sections, Cassing (1988) tentatively suggests the assumption that an equal number of nucleons from the projectile and the target contribute to emission (even in the case of asymmetric systems) so, for instance, in the case of neutron emission, assuming N_p to be the number of neutrons in the projectile, one gets

$$\frac{d^2N}{dEd\Omega} = \frac{2N_p f_{lab}(E,\Omega,t=\infty)}{\int d\mathbf{k} f_{av}(\mathbf{k},t=0)}. \qquad (7)$$

Some examples of the agreement between the data and this theory are shown in Fig. 7, 8, 9. In all cases the estimated theoretical yield has been reduced to one half to

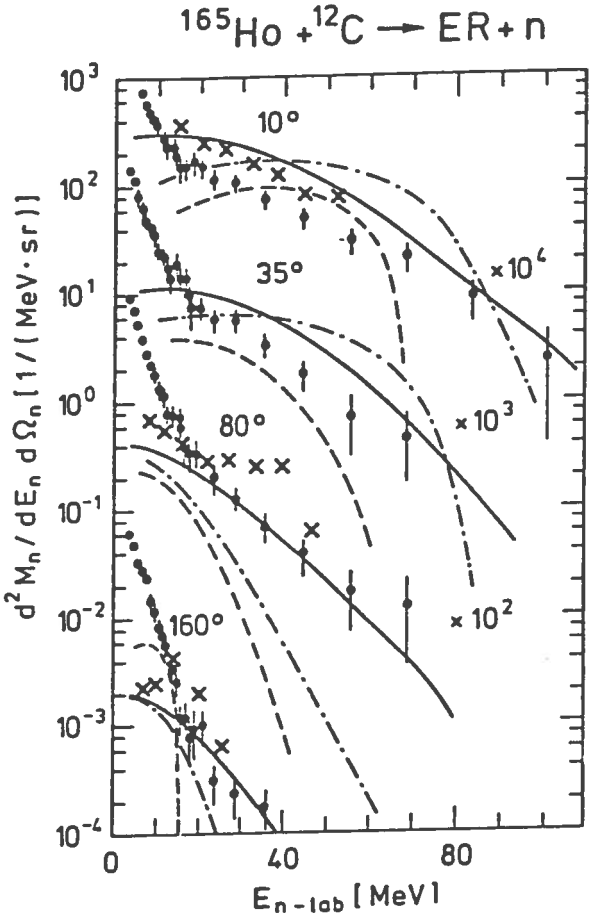

Fig. 7

Double differential multiplicity spectra of neutrons, in coincidence with an evaporation residue, emitted in the interaction of ^{12}C with ^{165}Ho at 600 MeV (Holub *et al* (1986). The continuous line is the result of calculations by Cassing (1988), the dashed line of Fermi jet calculations by Holub *et al* (1986), the dash-dotted line the result of using $f_{av}(\mathrm{k}, t = 0)$ given by two shifted Fermi gases at zero temperature (Cassing 1988).

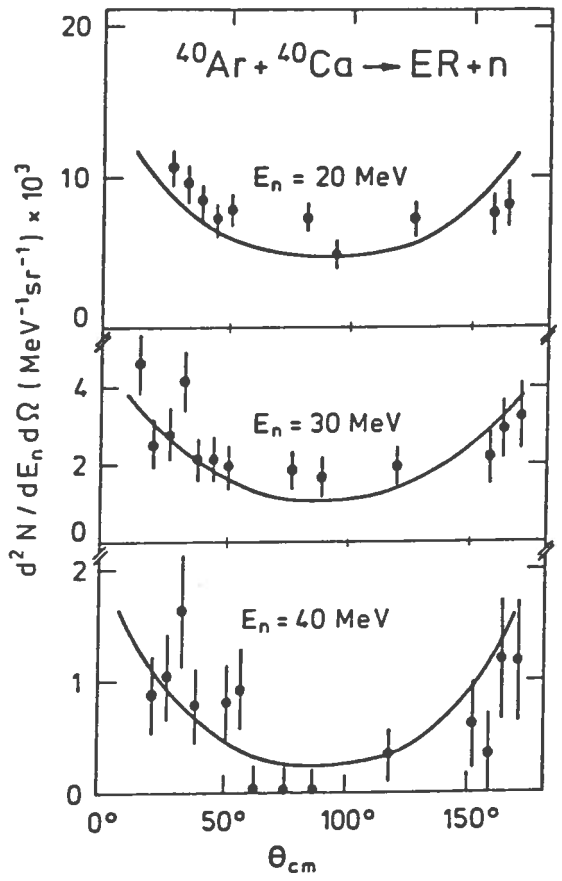

Fig. 8

Angular distributions of neutrons detected in coincidence with a forward emitted evaporation residue in the interaction of ^{40}Ar ions with ^{40}Ca ions (Rösch *et al* 1987). The continuous lines represent the prediction of the quantal phase space theory of Cassing (1988) where the theoretical yield has been divided by two as explained in the text.

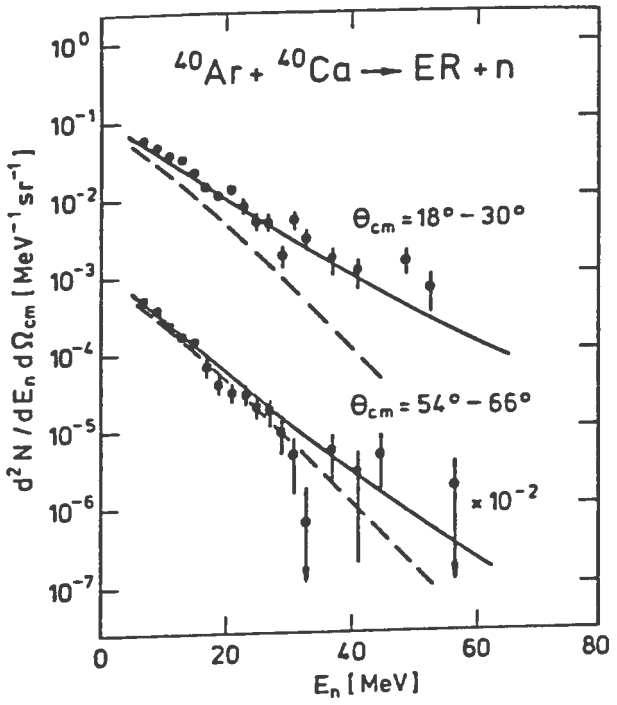

Fig. 9

Double differential spectra of neutrons, in coincidence with an evaporation residue, emitted in the ineteraction of ^{40}Ar with ^{40}Ca (Rösch *et al* 1987). The solid line is the sum of the pre-equilibrium component estimated by Cassing (1988) (and divided by two, as explained in the text) and an isotropic equilibrium component (Cassing 1988).

take into account the part of the calculated outgoing neutron flux that contributes to complex particle yield and has to be subtracted before comparison with experiment (this might be subject to some criticism since to take into account formation of complex particles one should increase the nucleon-nucleon interaction cross-section including a sticking term).

The effect of the mean field is also taken into account macroscopically by evaluating the trajectory of the two colliding ions under the action of Coulomb, nuclear (proximity interaction) and centrifugal forces. The so called one-body dissipation process occurs by means of a friction force or by exchange of nucleons through the neck that forms between the two nuclei when they come in close contact (Leray *et al* 1985, Randrup and Vandenbosch 1987). A window forms through the neck and fast nucleons with high momenta (originating, as already indicated, from the coupling of the translational momentum, due to their participating in the collective motion of the ion, and the internal Fermi-gas momentum) may transfer from the donor to the receptor propagating through the nuclear medium and being eventually emitted if they reach the receptor surface with sufficient energy to overcome the potential barrier. Randrup and Vandenbosch (1987) use the nucleon-exchange transport model to describe the two ion trajectories, the formation of the di-nucleus and the exchange of nucleons through the neck, (Randrup 1979, 1983, Dossing and Randrup 1985). The two ions are described as two Fermi gases with a sharp surface in coordinate space connected, when in close contact, by a neck of radius c_{eff}. When nucleon transfer from donor to receptor occurs the two nuclei are finite temperature Fermi gases, that have been heated by previous transfers and equilibrated. The transferred nucleon may experience a two-body interaction with a receptor nucleon and the collision probability per unit time is calculated as in pre-equilibrium phenomenological models as

$$W_{1p} = <\rho\sigma_{NN}^{eff} v_{rel} f_1' f_2'> \propto \int \frac{d\mathbf{p}_2}{h^3} f(\mathbf{p}_2)\sigma_{NN}^{eff}(E_{rel}) v_{rel} \overline{f}(\mathbf{p}_1')\overline{f}(\mathbf{p}_2'), \qquad (8)$$

where σ_{NN}^{eff} is the effective nucleon-nucleon cross section in nuclear matter, assumed equal to $k(=1/2)$ times the free nucleon nucleon cross-section, v_{rel} and E_{rel} are,

respectively, the two-nucleon relative velocity and energy and the indices 1 and 2 refer to the transferred and the receptor nucleons, and the primed quantities to the nucleons after the scattering. The quantities $\overline{f} \equiv (1 - f)$ represent the probability that the final state be available. Whenever a nucleon-nucleon collision occurs the propagation through the receptor of both the scattering partners is followed. When a nucleon reaches the receptor surface it escapes with a probability equal to the quantal transmission coefficient appropriate to the diffuse potential step and the refraction at the crossing of the nuclear surface is evaluated classically. The calculation is made for each partial wave contributing to a particular reaction.

The time evolution of a typical collision, predicted by these calculations, is shown in Fig. 10 that shows, from top to bottom, as a function of time (in units of 10^{-22} sec), in the case of the interaction of 402 MeV ^{20}Ne ions with ^{165}Ho and the l=46 partial wave, (a) the decrease of the radial component of the kinetic energy, (b) the variation of the internuclear separation R and the neck radius c_{eff}, (c) the evolution of the equilibrium temperatures of the projectile-like and the target-like di-nuclear components and, finally (d) the time-dependent multiplicity of the projectile nucleons emitted.

This figure shows that, according to the model, fast nucleon emission occurs after substantial damping of the two-nuclei kinetic energy, shortly after the neck formation, and when the temperature of the projectile-like fragment has almost reached its maximum value. The fact that the projectile may be described, at the moment of nucleon transfer, as a finite temperature Fermi gas leads to a substantial increase of the energy of emitted nucleons due to the coupling of the translational momentum with high internal motion momenta from the tail of the finite temperature Fermi-Dirac distribution.

In Fig. 11 (for the same reaction considered in Fig. 10) are shown the double-differential distributions predicted for the emitted neutrons (i) considering zero temperature donor nuclei and neglecting two-body interactions of the transferred nucleons (dashed lines), (ii) considering finite temperature donor nuclei (long dashed lines), and (iii) considering also the effect of two-body interactions (full lines). The

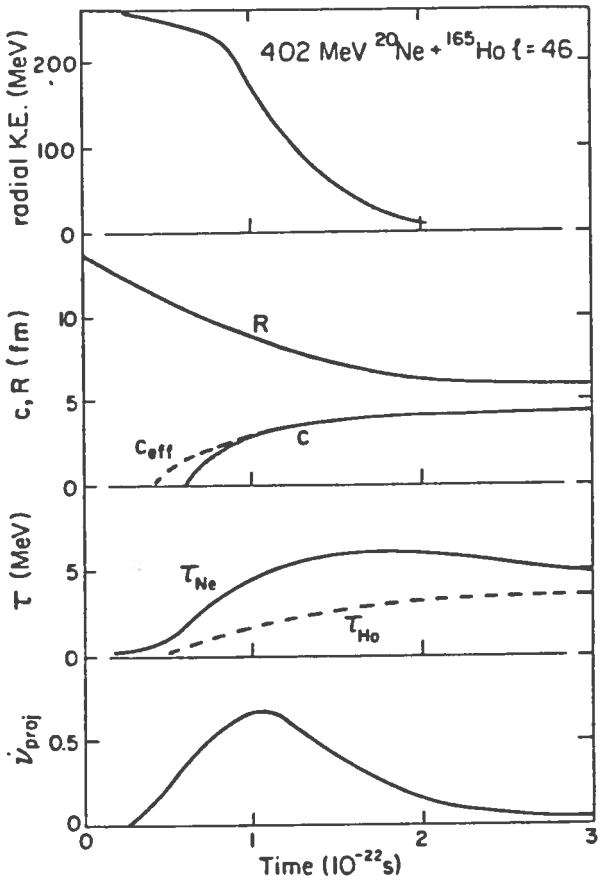

Fig. 10

Time evolution, according to Randrup and Vandenbosch (1987), of quantities relating to a typical collision between two heavy ions at an energy of $\approx$ 20 MeV/nucleon. For details, see the text.

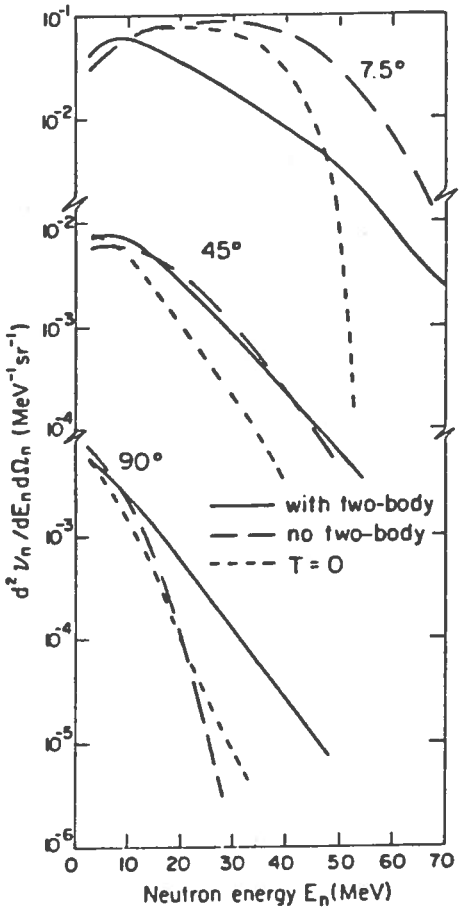

Fig. 11

Dependence, on model assumptions, of the calculated double differential neutron spectra for the interaction of ^{20}Ne ions with ^{165}Ho at 402 MeV. Dashed lines, zero temperature donor nuclei and absence of two-body interactions; long dashed lines, finite temperature donor nuclei; solid lines, finite temperature donor nuclei and two-body interactions (Randrup and Vandenbosch 1987).

increase of fast neutron emission at backward angles, considering finite temperature Fermi gases and two-body interactions, may be easily noted. Fig. 12 shows a typical fit to observed differential cross-sections (Randrup and Vandenbosch 1987).

All the approaches previously described take into account, to a different degree of accuracy, the so called one-body dissipation mechanism, due to the mean field acting on the interacting ions, and the two-body dissipation mechanism occurring *via* two-body nucleon-nucleon interactions. A number of calculations of nucleon spectra has also appeared in literature considering explicitly only the two-body interaction mechanism and these are more directly related to the calculations of pre-equilibrium cross-sections made in the case of light projectiles (Blann 1981, 1987, Blann and Remington 1988, Cindro 1988, Fabrici *et al* 1989a,b, Iwamoto 1987, Korolija *et al* 1988a, Remington *et al* 1988).

The justification of such procedures rests on the observation (Kruse *et al* 1985, Cassing 1987b) that for reaction times smaller than ≈ 30 fm/c$\approx 10^{-22}$ sec the colliding nucleon momentum distribution is not greatly changed by the mean field interaction.

Most of these calculations are based on the solution of a system of master equations proposed by Harp, Miller and Berne in 1968 for a one fermion gas and further generalised to two fermion gases by Harp and Miller in 1971.

In this theory (see Fig. 13) the nucleon states are classified according to their energy, ϵ, and divided into bins of width $\Delta\epsilon$. The number N_i of occupied states within each bin is equal to the product of the total number of states for that bin, g_i, times an occupation number $0 \leq n_i \leq 1$. Nucleons in states within bins i and j may interact and scatter to states within bins l and m subject to the conservation of energy and the availability of unoccupied states in l and m . Unbound nucleons may also escape from the nucleus with energy $\epsilon_i' = \epsilon_i - \epsilon_F - B_i$ (ϵ_F and B_i are, respectively, the Fermi energy and the binding energy of the nucleon in the composite nucleus) thus contributing to precompound emission.

The relaxation of the nucleus, is described by the master equations (written, in the following, for the proton gas, those for the neutron gas being the same with

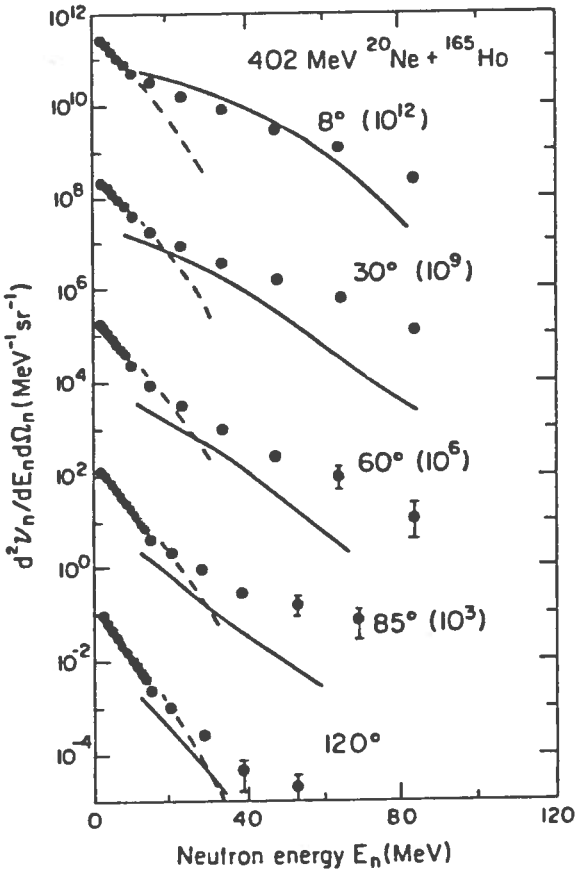

Fig. 12

Comparison of experimental double differential distributions of neutrons from the interaction of 402 MeV ^{20}Ne with ^{165}Ho (Holub *et al* 1983) with the theoretical predictions by Randrup and Vandenbosch (1987). The solid line give the calculated pre-equilibrium component, the dashed line the evaporative component (Randrup and Vandenbosch 1987).

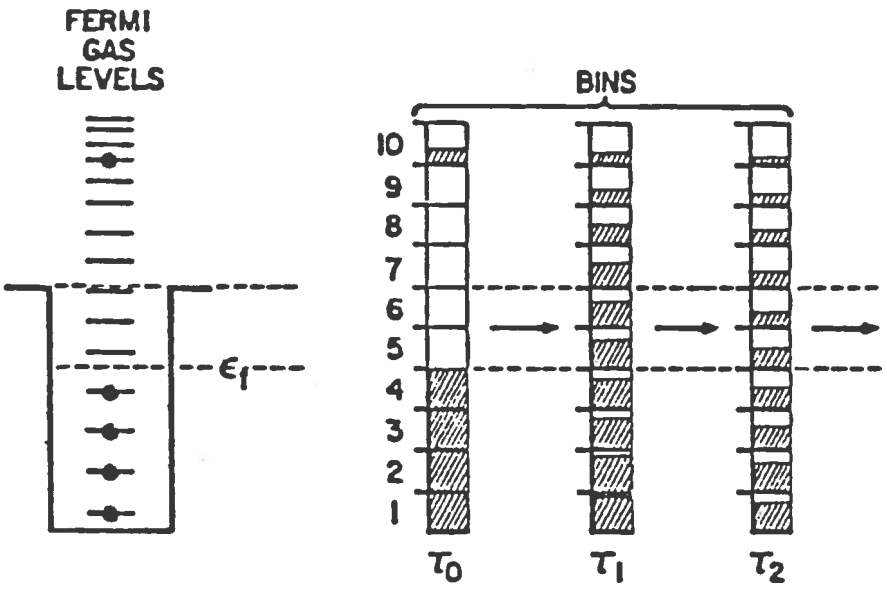

Fig. 13

Schematic representation of the time evolution of the occupation probability of single nucleon energy bins in a nucleon induced reaction according to Harp, Miller and Berne (Blann 1975)

obvious substitutions):

$$\frac{d(n_i g_i)^\pi}{dt} = \sum_{jlm}[\omega^{*,\pi\pi}_{lm\to ij} g_l^\pi n_l^\pi g_m^\pi n_m^\pi (1-n_i^\pi)(1-n_j^\pi) +$$

$$-\omega^{*,\pi\pi}_{ij\to lm} g_i^\pi n_i^\pi g_j^\pi n_j^\pi (1-n_l^\pi)(1-n_m^\pi)] + \sum_{jlm}[\omega^{*,\pi\nu}_{lm\to ij} g_l^\pi n_l^\pi g_m^\nu n_m^\nu (1-n_i^\pi)(1-n_j^\nu) +$$

$$-\omega^{*\pi\nu}_{ij\to lm} g_i^\pi n_i^\pi g_j^\nu n_j^\nu (1-n_l^\pi)(1-n_m^\nu)] - n_i^\pi g_i^\pi \omega^\pi_{i\to i'} g_{i'}^\pi \delta(\epsilon_i^\pi - \epsilon_F^\pi - B_i^\pi - \epsilon_{i'}^\pi), \quad (9)$$

and emission of particles to the continuum is obtained by integrating the equations

$$\frac{dN_i'^\pi}{dt} = n_i^\pi g_i^\pi \omega^\pi_{i\to i'} g_{i'}^\pi \delta(\epsilon_i^\pi - \epsilon_F^\pi - B_i^\pi - \epsilon_{i'}^\pi). \quad (10)$$

The quantities $\omega^*_{ij\to lm}$ are the decay rate for the scattering of particles in definite states of the bins i and j to bins l and m (evaluated as discussed by Fabrici *et al* 1989b) and

$$\omega_{i\to i'} = \frac{\sigma_{inv} v_{i'}}{g_i \Omega} \quad (11)$$

are the decay rates for emission of particles into the continuum. The quantities σ_{inv}, $v_{i'}$ and Ω are respectively the inverse cross-section, the emitted nucleon velocity and the Lab. volume which cancels a similar factor appearing in the expression for $g_{i'}$.

The system of master equations (9) is not the original one proposed by Harp *et al* but that proposed by Fabrici *et al* (1989b) obtained by eliminating two of the approximations made by Harp *et al* in evaluating the decay rates for nucleon-nucleon interactions, namely that of considering only perpendicular collisions which is inconsistent with the assumption of energy-dependent nucleon-nucleon cross sections, and that of considering as equiprobable any partition of initial energy between the final particles provided that their total energy is conserved. In fact linear momentum conservation leads to further restrictions on the possible values of the energies of the particles after scattering.

Most of these last calculations have been made by Blann and collaborators (Blann 1981, 1987, Blann and Remington 1988 and references therein) who analysed exclusive spectra of nucleons in coincidence with evaporation residues with a modified set

of Harp, Miller and Berne master equations (Blann 1981) assuming the initial excitation energy partitioned statistically among the projectile nucleons while the target was considered to be a Fermi gas at zero temperature.

The modified master equations used by Blann contain in addition to the terms appearing in (9) an injection term $[d(N_i(t)/dt]_{fus}$ $(N_i(t) = n_i g_i)$ that should describe the time-dependent rate of insertion, into the coalescing system, of nucleons of a given energy (bin i) coming from the projectile (assumed to be the lighter nucleus).

These calculations often provide excellent reproductions of angle integrated particle spectra, however the use of an initial exciton energy distribution corresponding to a statistical partition of the energy does not seem consistent with the momentum space description of the dynamics of the interaction process considered in all previously discussed theories. In fact it is straightforward to evaluate the particle and hole initial distribution resulting from the assumption of the coupling of the translational momentum of the nucleons (due to their being part of a translating ion) and their Fermi motion momentum, and it is found that it does not coincides with the statistical distribution. Fig. 14 shows the occupation probability distribution of the neutron states of the composite nucleus available per unit energy bin, in the case of the interaction of (a) 600 MeV ^{20}Ne ions with ^{165}Ho (dashed line) and (b) 800 MeV ^{40}Ar ions on ^{40}Ca (continuous line) (Fabrici *et al* 1989b). The calculation is made using a value of 40 MeV for the Fermi energy of projectile, target and composite nucleus, assuming a central collision and that the Coulomb potential energy of the two ions is converted back into translational kinetic energy as they fuse. These distributions are characterized by holes, in addition to excited particles, whose number and excitation energy depends on the projectile-target mass symmetry. The presence of these holes allows, as the cascade of nucleon-nucleon collisions develops, the excitation of particles to an energy higher than that resulting from the coupling of the internal and translational momenta.

Fabrici *et al* (1989b) have investigated quantitatively this effect using the Harp, Miller and Berne master equation theory. In case of very asymmetric systems like C or Ne + Ho, the calculated spectrum closely resembles that obtained by means of a

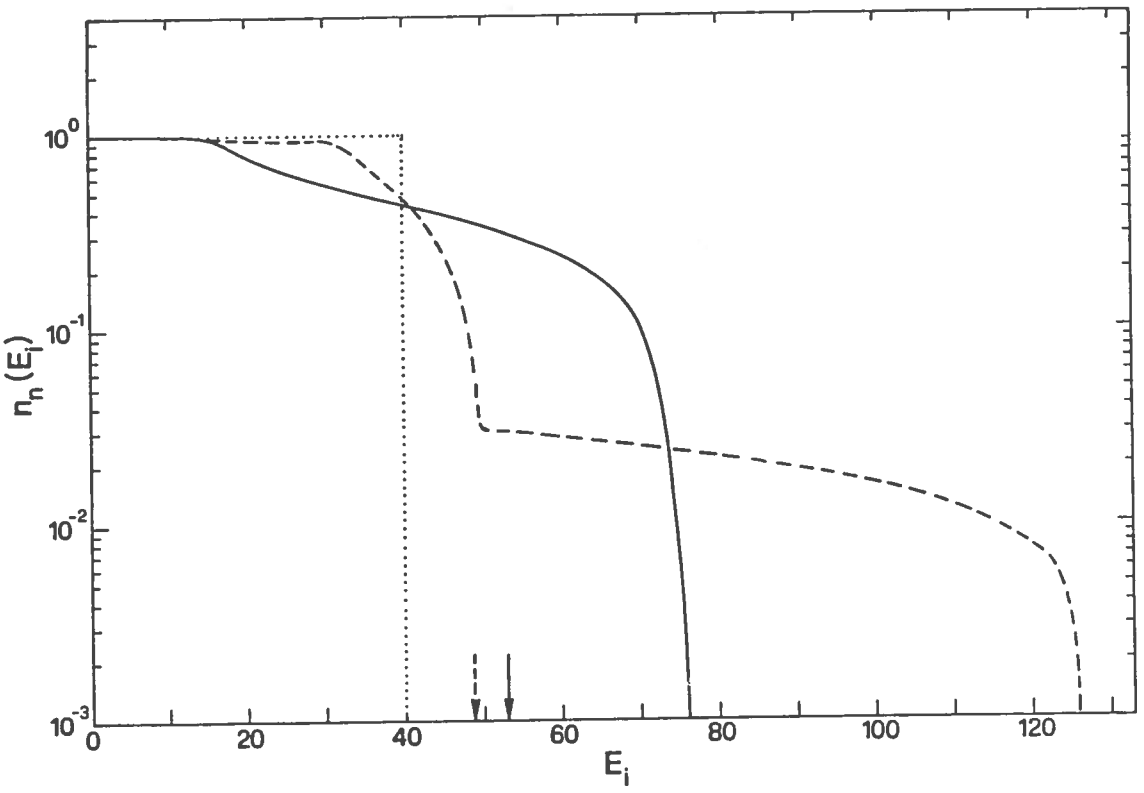

Fig. 14

Occupation number distribution of neutron states of the composite nucleus, at the beginning of the de-excitation cascade, in the case of 600 MeV ^{20}Ne ions on ^{165}Ho (dashed line) and 800 MeV ^{40}Ar on ^{40}Ca (full line). Neutrons with energy in excess of, respectively, the dashed and the full arrow are in the continuum. The dotted line gives the occupation number distribution for a zero temperature Fermi gas (Fabrici *et al* 1989b).

generalisation of the exciton model (Fig. 15, Fabrici *et al* 1989a) which consists in neglecting the hole excitations and in considering simply the excited particles that in the case of very asymmetric systems are essentially the projectile nucleons. This demonstrates that for asymmetric systems like those above considered (asymmetry parameter $y = A_p/A_T \leq 0.13$) the effect of interactions between excited nucleons in the presence of deep holes is of negligible importance. Basically different is the result one finds when one considers a symmetric system ($y = 1$) such as ^{40}Ar + ^{40}Ca at 800 MeV. In this case, the maximum neutron energy at the beginning of the nucleon-nucleon interaction cascade, corresponding to the kinematical limit $E_K = (p_t + p_F)^2/2m_n - B - \epsilon_F$ (where p_t and p_F are the translational and the Fermi momentum; B, ϵ_F and m_n are, respectively, the neutron binding energy, the Fermi energy and the nucleon mass), is only ≈20.3 MeV, an energy considerably smaller than that to which the experimental neutron spectrum measured by Rösch *et al* (1987) extends. Also considering the smearing due to the low energy resolution affecting these data, one cannot bring the calculations in agreement with the data in the absence of a considerable hardening of the spectrum due to nucleon-nucleon collisions. The comparison in Fig. 16 of the experimental neutron spectrum (Lassen 1988) (thick full line) with the ones calculated using free nucleon-nucleon cross-sections (thin full line) and cross-sections scaled, respectively, by a factor 2 (dashed line) and 4 (dotted line) shows that this hardening occurs. The calculated spectra are in excellent agreement with the measured spectrum thus showing that nucleon-nucleon interactions have considerably hardened the neutron energy distribution existing at the beginning of the nucleon-nucleon interaction cascade.

The importance of nucleon-nucleon interactions is also indicated by the dependence of the calculated neutron yield on the scaling factor multiplying the free nucleon-nucleon cross-section. In this case, at variance with that which occurs in the case of very asymmetric systems, a larger nucleon-nucleon cross-section results in an increased yield of high energy neutrons. An increase of the interaction cross-section increases the probability of producing high energy nucleons in nucleon-nucleon interactions. At the same time, the probability of their emission into the continuum

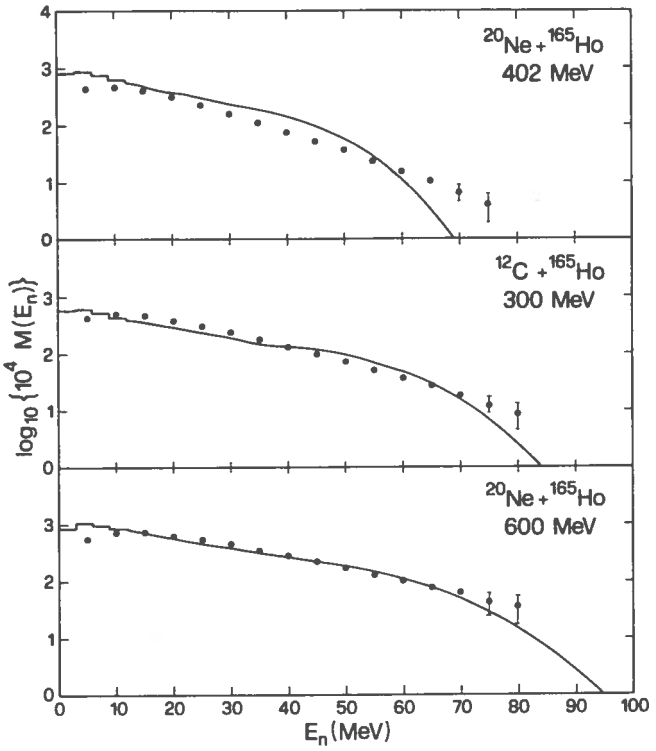

Fig. 15

Angle integrated centre of mass multiplicity distributions of pre-equilibrium neutrons for the reactions indicated. The experimental results are given by the solid dots, the theoretical expectations by the solid lines (Fabrici *et al* 1989a).

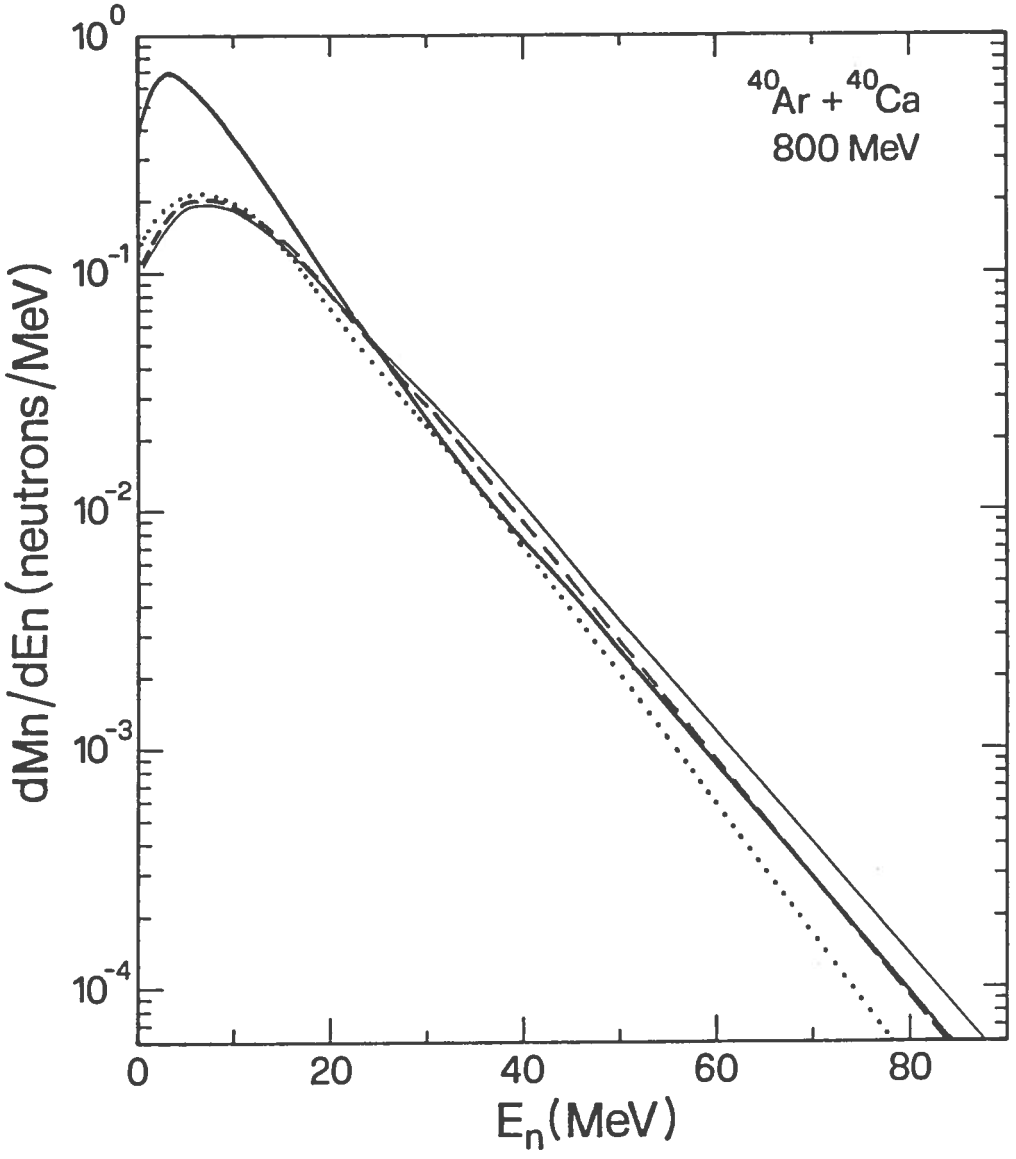

Fig. 16

Comparison of the neutron spectrum from the interaction of 800 MeV ^{40}Ar ions with $^{40}Ca^{25}$ (thick full line, Lassen 1988) with the spectra calculated using free nucleon-nucleon cross-sections (thin full line) and cross-sections scaled, respectively, by a factor 2 (dashed line) and 4 (dotted line) (Fabrici *et al* 1989b).

decreases. The emitted nucleon yield depends on both these two opposite tendencies and the observed increase in the yield of the emitted neutrons for a larger nucleon-nucleon cross-section demonstrates that the first effect is predominant. The calculations by Cassing (1988) do not reveal this hardening of the initial nucleon spectra due to fast nucleon interactions in presence of deep holes, as it is demonstrated by Fig. 17 which shows that, in his calculations, an increase of the nucleon-nucleon interaction cross section leads to a decrease of fast neutron emission even in the case of symmetric heavy ion interactions.

In the case of very asymmetric systems the amount of high energy nucleons at the beginning of the interaction cascade is too small to produce any significant yield of high energy nucleons as a result of the nucleon-nucleon interactions and, in practice, the second effect is the only one operating. Thus, an increase of the nucleon-nucleon cross-section reduces the yield of high energy neutrons.

In Fig. 18 are shown, for systems of different symmetry ((A) ^{32}S + ^{27}Al ($y = .84$, full line), (B) ^{32}S + ^{58}Ni ($y = .55$, dotted and dashed line), (C) ^{32}S + ^{120}Sn ($y = .27$, dotted line), (D) ^{32}S + ^{197}Au ($y = .16$, dashed line)), the calculated spectra of pre-equilibrium protons at a time $\approx 2 \cdot 10^{-22}$ sec from the beginning of the nucleon-nucleon interaction cascade. The energy of the incident ^{32}S ion beam is in all cases equal to 679 MeV and, in the calculation, free nucleon-nucleon cross sections have been used. The arrows indicate, in each case, the highest energy of the protons at the beginning of the interaction cascade resulting from the kinematical coupling of the translational and internal momentum. The importance of the nucleon-nucleon interaction is shown by the fact that, in spite of the considerably different initial energy distributions the emitted particle spectra are very similar and, if there is a difference, the softest spectrum corresponds to the hardest initial distribution. In case (D) one may identify two components of the calculated spectrum, one corresponding to the particles emitted immediately, without any interaction, that ends at the energy corresponding to the arrow (D), and one of protons that acquired energy in at least one previous nucleon-nucleon interaction. The two contributions are barely observable in the case of ^{120}Sn, and cannot be separated in all the other cases.

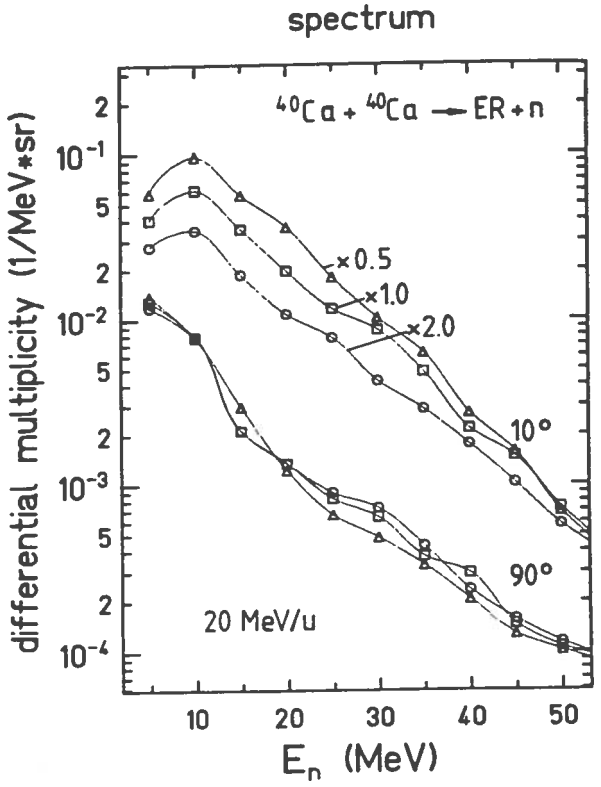

Fig. 17

Double differential pre-equilibrium neutron multiplicities for central collisions of ^{40}Ca on ^{40}Ca at 20 MeV/nucleon, calculated by Cassing (1988) using free nucleon-nucleon cross-sections (open squares), and free nucleon-nucleon cross-sections multiplied by, respectively, 2 (open circles) and 0.5 (open triangles).

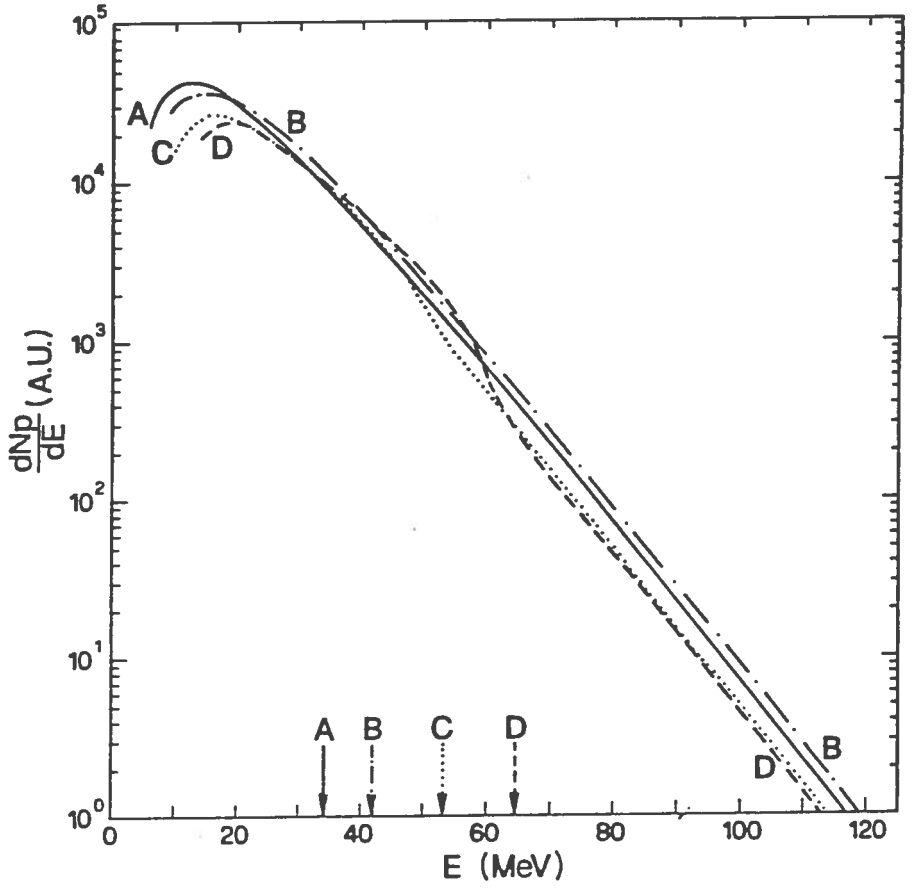

Fig. 18

Calculated proton spectra (after a time $T \approx 2 \cdot 10^{-22}$ sec) from the beginning of nucleon-nucleon interaction cascade, resulting from the interaction of (A) ^{32}S and ^{27}Al ($y = .84$), (B) ^{32}S and ^{58}Ni ($y = .55$), (C) ^{32}S and ^{120}Sn ($y = .27$), (D) ^{32}S and ^{197}Au ($y = .16$). The energy of the incident ^{32}S ion beam is, in all cases, equal to 679 MeV, and free nucleon-nucleon cross-sections have been used in the calculation. The arrows indicate, in each case, the highest possible energy of protons at the beginning of the interaction cascade resulting from the kinematical coupling of the translational and internal momentum of either the projectile or the target (Fabrici *et al* 1989b).

The hardening of the nucleon spectrum obviously depends on the probability of interaction of two particles of sufficient high initial energies ϵ_i and ϵ_j which is proportional to the product of the corresponding number of occupied states $n_i g_i \cdot n_j g_j$ and the availability of deep holes at energy ϵ_l where one of the two particles may scatter, which is proportional to $(1 - n_l)$. The comparison, in Fig. 14, of the initial occupation number distributions corresponding to asymmetric system Ne + Ho and to the symmetric system Ar + Ca shows that the probability of a nucleon-nucleon interaction producing nucleons with energy greater than that of the interacting nucleons may be orders of magnitudes greater in the symmetric case.

To conclude, it has been shown that, starting from incident energies of the order of a few ten MeV/nucleon ($\approx$ 20 MeV/nucleon) nucleon-nucleon collisions play a major role in the equilibration process of the di-nuclear system created in the interaction of two heavy ions. These interactions also influence in a significant way the energy and angular distribution (in addition to the absolute yield) of fast nucleons emitted at an early stage of the two-ion interaction process. They might even lead to a considerable hardening of the primary nucleon spectrum when the symmetry parameter y is sufficiently high ($\geq\approx .15$).

We wish to thank Elsa Fabrici, Franca Fabbri, Marina Galmarini and Gianni Reffo for their allowing extensive quotation from a paper written together with them and for their invaluable help and advice, and to Peter E. Hodgson for a careful reading of the manuscript and many enlightening suggestions.

Aichelin J and Bertsch G 1985 Phys. Rev. **C31** 1730

Aichelin J 1986 Proceedings of the *International Conference on Heavy-ion Nuclear Collisions in the Fermi Energy Domain* Caen (France), May 12-16, 1986, Editions de Physique: Les Ulis (France)

Awes T C, Poggi G, Gelbke C K, Back B B, Glagola B G, Breuer H and Viola V E jr. 1981 Phys. Rev. **C24** 89

Awes T C, Saini S, Poggi G, Gelbke C K, Cha D, Legrain R and Westfall G D 1982

Phys. Rev. **C25** 2361

Blann M 1981 Phys. Rev. **C23** 205

Blann M 1987 Phys. Rev. **C35** 1581

Blann M and Remington B A 1988 Proceedings of the Varenna Conference, Edt. E. Gadioli, Ricerca Scientifica ed Educazione Permanente, Suppl. n. **66** 184

Bondorf J B, De J N, Fai G, Karvinen A O T, Jakobsson B and Randrup J 1980 Nucl. Phys. **A333** 285

Cassing W 1987a Z. Phys. **A327** 87

——1987b Z. Phys. **A327** 447

——1988 Z. Phys. **A329** 471

Cindro N 1988 Proceedings of the Varenna Conference, Edt. E. Gadioli, Ricerca Scientifica ed Educazione Permanente, Suppl. n. **66** 194

Collins M T and Griffin J J 1980 Nucl. Phys. **A34** 863

Davies K T R, Devi K R S, Koonin S E and Strayer M R 1984 *Heavy-ion Science*, D. A. Bromley Edt., Plenum: New York

Dossing T and Randrup J 1985 Nucl. Phys. **A433** 215

Fabrici E, Gadioli E and Gadioli Erba E 1989a, Phys. Rev. **C40** 459

Fabrici E, Gadioli E, Gadioli Erba E, Galmarini M, Fabbri F and Reffo G 1989b *submitted for publication*

Glasow R, Gaul G, Ludewigt B, Santo R, Ho H, Kühn W, Lynen U and Müller W F J 1983 Phys. Lett. **120B** 71

Harp G D, Miller J M and Berne B J 1968 Phys. Rev. **165** 1166

Harp G D and Miller J M 1971 Phys. Rev **C3** 1847

Hilscher D, Rossner H, Gamp A, Jahnke U, Cheynis B, Chambon B, Drain D, Pastor C, Giorni A, Morand C, Dauchy A, Stassi P and Petitt G 1987 Phys. Rev. **C36** 208

Holub E, Hilscher D, Ingold G, Jahnke U, Orf H and Rossner H 1983a Phys. Rev. **C28** 252

Holub E, Hilscher D, Ingold G, Jahnke U, Orf H, Rossner H, Zank W P, Schröder W U, Gemmeke H, Keller K, Lassen L and Lücking W 1986 Phys. Rev. **C33** 143

Holub E, Korolija M and Cindro N 1983b Z Phys **A314** 347

Iwamoto A 1987 Phys. Rev. **C35** 984

Korolija M, Cindro N and Caplar R 1988a Phys. Rev. Lett. **60** 193

Korolija M, Cindro N, Caplar R, Auble R L, Ball J B and Robinson R L 1988b *Private communication, to be published*

Kruse H, Jacak B V, Molitoris J J, Westfall G D and Stöcker H 1985 Phys. Rev. **C31** 1770

Lassen N O 1988 Proceedings of the Varenna Conference, Edt. E. Gadioli, Ricerca Scientifica ed Educazione Permanente, Suppl. n. **66** 223

Leray S, La Rana G, Ngo C, Barranco M, Pi M and Vinas X 1985 Z. Phys. **A320** 383

Mantzouranis G, Weidenmüller H A and Agassi D 1976 Z. Phys. **A276** 145

Morison W W, Samaddar S K, Sperber D and Zielinska-Pfabe M 1980 Phys. Lett. **93B** 379

J. Negele 1982 Rev. Mod. Phys. **54** 913

Randrup J 1979 Nucl. Phys. **A327** 490

—— 1983 Nucl. Phys. **A383** 468

Randrup J and Vandenbosch R 1987 Nucl. Phys. **A474** 219

Remington B A, Blann M, Galonsky A, Heilbronn L, Deak F, Kiss A and Seres Z 1988 Phys. Rev. **C38** 1746

Robel M C 1979 Ph. D. Thesis, LBL-8181, *unpublished*

Rösch W, Richter A, Schrieder G, Gentner R, Keller K, Lassen L, Lücking W, Schreck R, Cassing and W, Gemmeke H 1987 Phys. Lett. **197B** 19